Pružný rozptyl, luminiscence, <u>Ramanův rozptyl</u>

v. 1c
16.12.2024

Josef Humlíček, humlicek@physics.muni.cz

- pružný a nepružný rozptyl fotonu
- objev Ramanova jevu
- fenomenologický popis, kvantové přechody

- ukázky spekter

Pružný (Rayleighův) rozptyl

Lord Rayleigh, 'Phil. Mag.,' vol. 47, p. 375 (1899)

XXXIV. *On the Transmission of Light through an Atmosphere containing Small Particles in Suspension, and on the Origin of the Blue of the Sky.* By Lord RAYLEIGH, F.R.S.*

THIS subject has been treated in papers published many years ago †. I resume it in order to examine more closely than hitherto the attenuation undergone by the primary light on its passage through a medium containing small particles, as dependent upon the number and size of the particles. Closely connected with this is the interesting

* Communicated by the Author.
† Phil. Mag. xli. pp. 107, 274, 447 (1871); xii. p. 81 (1881).

Pružný (Rayleighův) rozptyl – záření dipólu

For such a purpose as the present it makes little difference whether we speak in terms of the electromagnetic theory or of the elastic solid theory of light; but to facilitate comparison with former papers on the light from the sky, it will be convenient to follow the latter course. The small particle of volume T is supposed to be small in all its dimensions in comparison with the wave-length (λ), and to be of optical density D' differing from that (D) of the surrounding medium. Then, if the incident vibration be taken as unity, the expression for the vibration scattered from the particle in a direction making an angle θ with that of *primary vibration* is

$$\frac{D'-D}{D} \frac{\pi T}{r\lambda^2} \sin\theta \cos\frac{2\pi}{\lambda}(bt-r)^*, \quad . \quad . \quad . \quad (1)$$

r being the distance from T of any point along the secondary ray.

In order to find the whole emission of energy from T we have to integrate the square of (1) over the surface of a sphere of radius r. The element of area being $2\pi r^2 \sin\theta\, d\theta$, we have

$$\int_0^\pi \frac{\sin^2\theta}{r^2} 2\pi r^2 \sin\theta\, d\theta = 4\pi \int_0^{\frac{1}{2}\pi} \sin^3\theta\, d\theta = \frac{8\pi}{3};$$

so that the energy emitted from T is represented by

$$\frac{8\pi^3}{3} \frac{(D'-D)^2}{D^2} \frac{T^2}{\lambda^4}, \quad . \quad . \quad . \quad . \quad . \quad (2)$$

on such a scale that the energy of the primary wave is unity per unit of wave-front area.

Pružný (Rayleighův) rozptyl - experiment s čistým vzduchem

R. J. Strutt, 'Scattering of light by dust-free air, with artificial reproduction of the blue sky, *Proc. R. Soc. Lond.* A. **94** (1918), 453–459. R. J. Strutt inherited the title of Lord Rayleigh on the death of his father in 1919. While it is not formally correct to refer to him by title before 1919, the name Rayleigh is nowadays more widely recognized than the family name of Strutt.

It is now well established* that the luminosity and blue colour of the sky on very clear days and at considerable altitudes above the sea-level can almost be accounted for by the scattering of light by the molecules of air, without postulating suspended particles of foreign matter, such as were thought necessary by the earlier writers.

This conclusion depends on the measured opacity of the atmosphere, deduced from observations such as those of Abbot and Fowle† of the sun's radiation at various zenith distances. The opacities measured at Mount Wilson for different wave-lengths are found to be nearly in agreement with what would be expected if scattering by the molecules were alone operative; leaving little room for the action of larger particles.

Pružný (Rayleighův) rozptyl
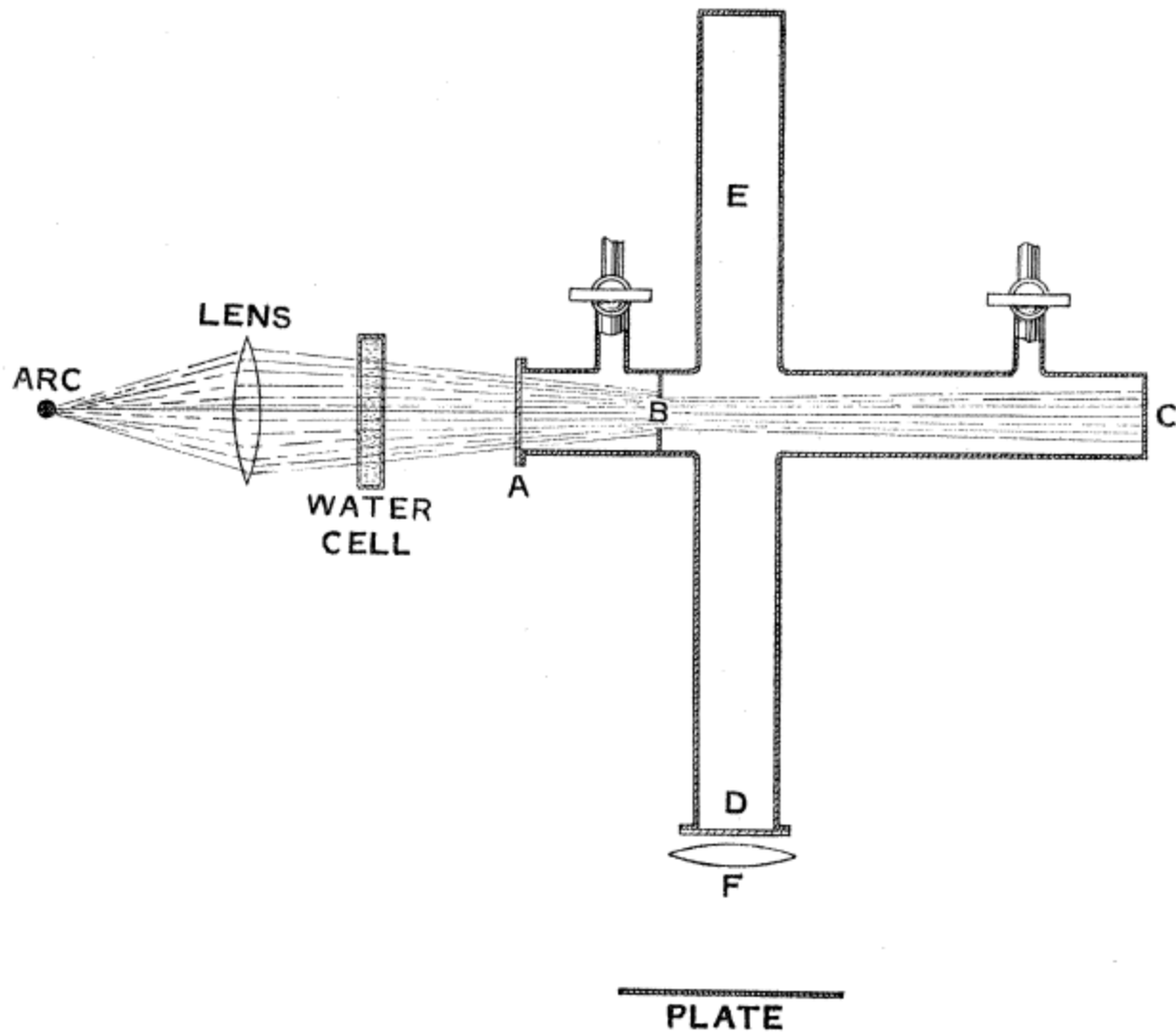
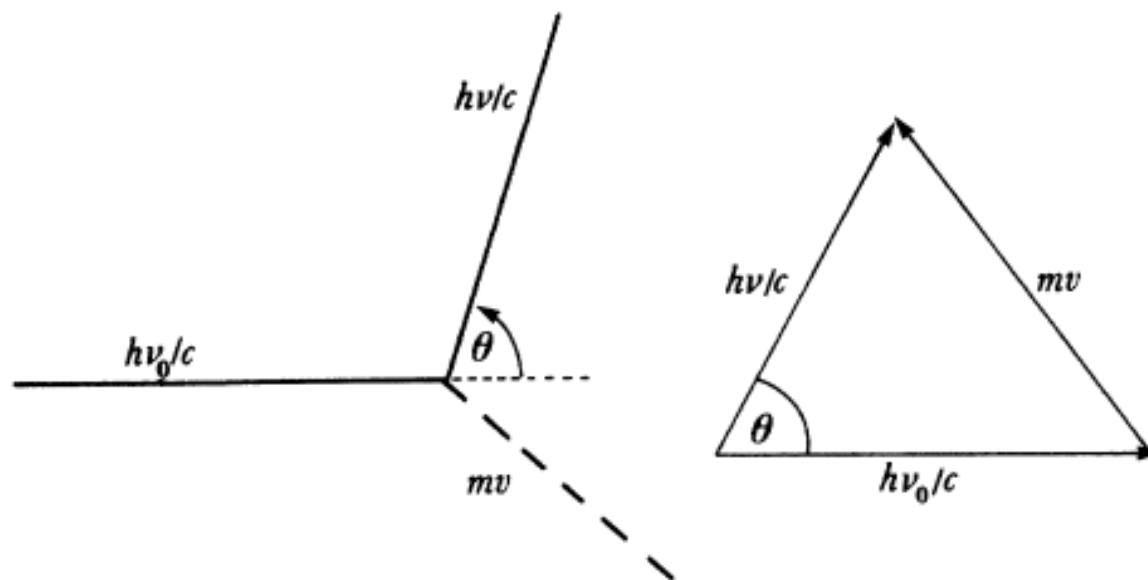Nepružný rozptyl rtg záření (Comptonův rozptyl)

FIGURE 2. The Compton effect. An X-ray photon of frequency ν_0, energy $h\nu_0$ and momentum $h\nu_0/c$ is deflected by collision with an electron (mass m) which recoils with velocity ν. Radiation reflected, or *scattered*, at θ to the incident beam is characterized by a shifted frequency ν. In Brillouin scattering of visible or ultraviolet light the broken line defines the track of the acoustic quantum, or *phonon*, of energy $h\nu_s$ and momentum $h\nu_s/V = h/\Lambda$, where ν_s is the frequency and Λ the wavelength of sound in the medium.

THE
PHYSICAL REVIEW

THE SPECTRUM OF SCATTERED X-RAYS[1]

By Arthur H. Compton

Abstract

The spectrum of molybdenum Kα rays scattered by graphite at 45°, 90° and 135° has been compared with the spectrum of the primary beam. A primary spectrum line when scattered is broken up into two lines, an "unmodified" line whose wave-length remains unchanged, and a "modified" line whose wave-length is greater than that of the primary spectrum line. Within a probable error of about 0.001 A, the difference in the wave-lengths $(\lambda - \lambda_0)$ increases with the angle θ between the primary and the scattered rays according to the quantum relation $(\lambda - \lambda_0) = \lambda(1 - \cos\theta)$, where $\lambda = h/mc = 0.0242$ A. This wave-length change is confirmed also by absorption measurements. The modified ray does not seem to be as homogeneous as the unmodified ray; it is less intense at small angles and more intense at large angles than is the unmodified ray.

An x-ray tube of small diameter and with a water-cooled target is described, which is suitable for giving intense x-rays.

Apparatus and method. For the quantitative measurement of the change in wave-length it was clearly desirable to employ a spectroscopic method. In view of the comparatively low intensity of scattered x-rays, the apparatus had to be designed in such a manner as to secure the maximum intensity in the beam whose wave-length was measured. The arrangement of the apparatus is shown diagrammatically in Fig. 1. Rays proceeded from the molybdenum target T of an x-ray tube to the graphite
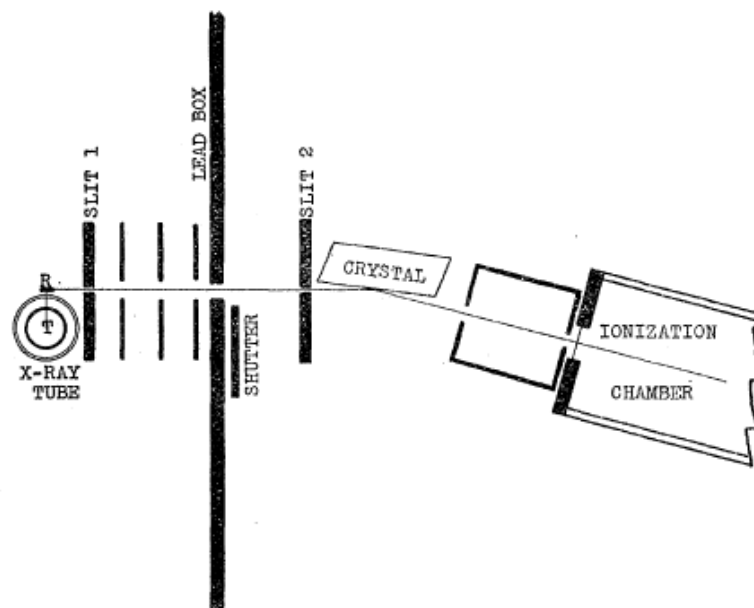

Fig. 1. Measuring the wave-length of scattered x-rays.

scattering block R, which was placed in line with the slits 1 and 2. Lead diaphragms, suitably disposed, prevented stray radiation from leaving the lead box that surrounded the x-ray tube. Since the slit 1 and the diaphragms were mounted upon an insulating support, it was possible to place the x-ray tube close to the slit without danger of puncture. The x-rays, after passing through the slits, were measured by a Bragg spectrometer in the usual manner.

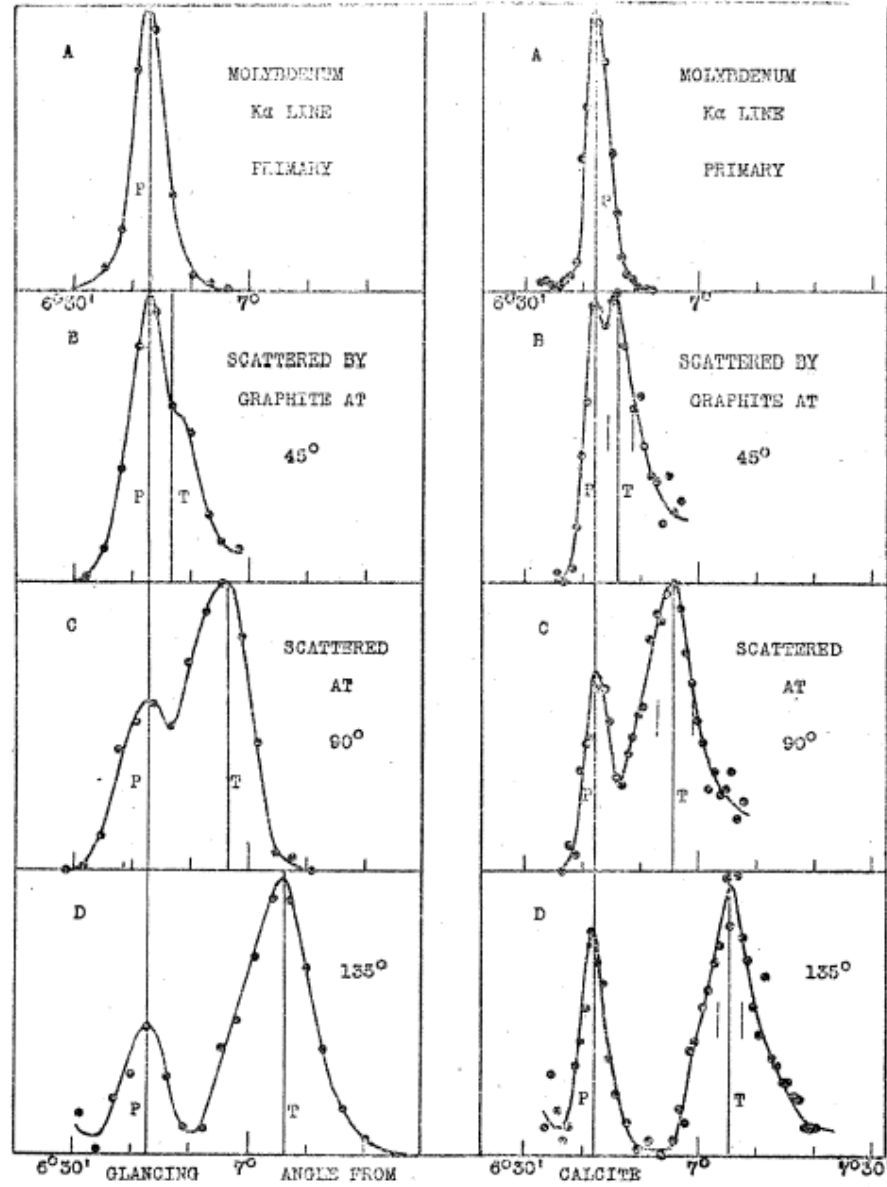# A. Compton 1923: částicové vlastnosti vlnění

Fig. 3

Fig. 4

Nepružný rozptyl světla na nehomogenitách (např. akustických fononech)
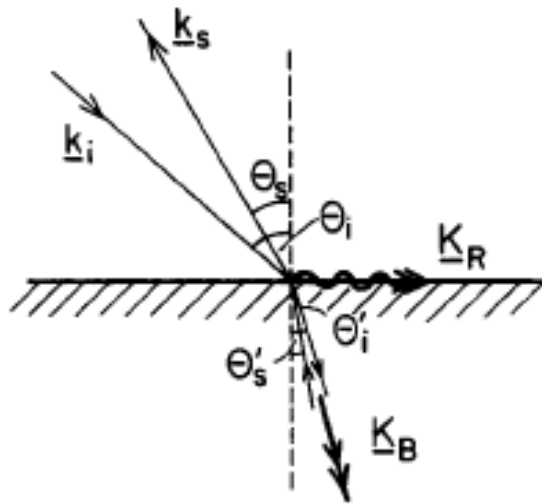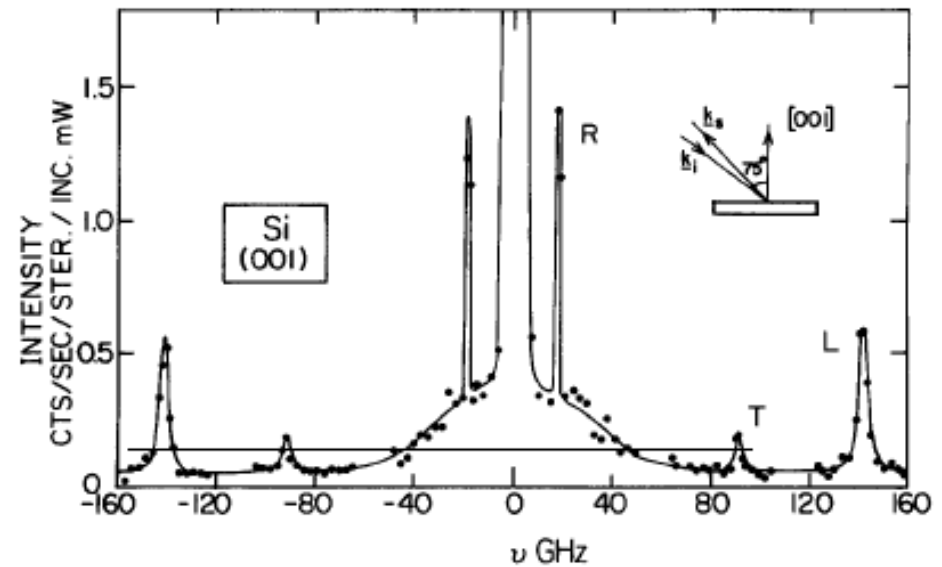předpověď Brillouin 1922

Snadercock 1978 (Si, Ge)

Fig. 1. Geometry of the experiment showing incident and scattered light wavevectors k_i and k_s and the surface and bulk phonon wavevectors K_R and K_B.

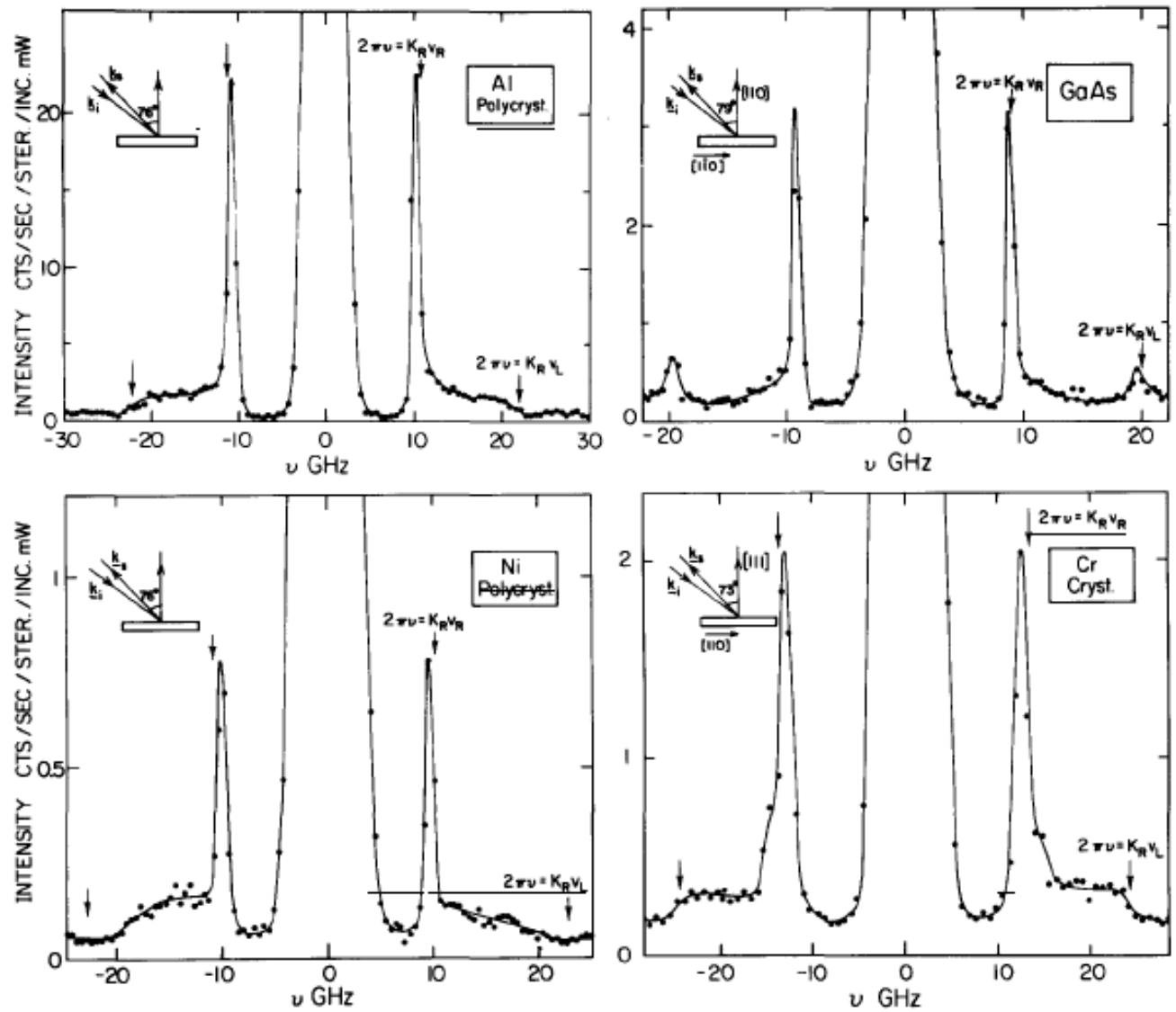Sandercock 1978 (kovy, polovodiče)

Fig. 4. Representative spectra taken with the tandem interferometer for crystalline Cr and GaAs, and polycrystalline Al and Ni. Note the high energy shoulder on the surface phonon peaks.

Nepružný rozptyl viditelného světla - Raman & Krishnan , Nature1928
1930 Nobelova cena (Raman)

C. V. RAMAN.
K. S. KRISHNAN.

210 Bowbazar Street,
Calcutta, India,
Feb. 16.

IF we assume that the X-ray scattering of the 'unmodified' type observed by Prof. Compton corresponds to the normal or average state of the atoms and molecules, while the 'modified' scattering of altered wave-length corresponds to their fluctuations from that state, it would follow that we should expect also in the case of ordinary light two types of scattering, one determined by the normal optical properties of the atoms or molecules, and another representing the effect of their fluctuations from their normal state. It accordingly becomes necessary to test whether this is actually the case. The experiments we have made have confirmed this anticipation, and shown that in every case in which light is scattered by the molecules in dust-free liquids or gases, the diffuse radiation of the ordinary kind, having the same wave-length as the incident beam, is accompanied by a modified scattered radiation of degraded frequency.

Nepružný rozptyl viditelného světla - Raman & Krishnan , Nature1928

The new type of light scattering discovered by us naturally requires very powerful illumination for its observation. In our experiments, a beam of sunlight was converged successively by a telescope objective of 18 cm. aperture and 230 cm. focal length, and by a second lens of 5 cm. focal length. At the focus of the second lens was placed the scattering material, which is either a liquid (carefully purified by repeated distillation *in vacuo*) or its dust-free vapour. To detect the presence of a modified scattered radiation, the method of complementary light-filters was used. A blue-violet filter, when coupled with a yellow-green filter and placed in the incident light, completely extinguished the track of the light through the liquid or vapour. The reappearance of the track when the yellow filter is transferred to a place between it and the observer's eye is proof of the existence of a modified scattered radiation. Spectroscopic confirmation is also available.

Nepružný rozptyl viditelného světla - Raman & Krishnan , Nature1928

Some sixty different common liquids have been examined in this way, and every one of them showed the effect in greater or less degree. That the effect is a true scattering and not a fluorescence is indicated in the first place by its feebleness in comparison with the ordinary scattering, and secondly by its polarisation, which is in many cases quite strong and comparable with the polarisation of the ordinary scattering. The investigation is naturally much more difficult in the case of gases and vapours, owing to the excessive feebleness of the effect. Nevertheless, when the vapour is of sufficient density, for example with ether or amylene, the modified scattering is readily demonstrable.

Ramanův „spektrograf" (Hilger), Hg výbojka + oko nebo fotografická deska
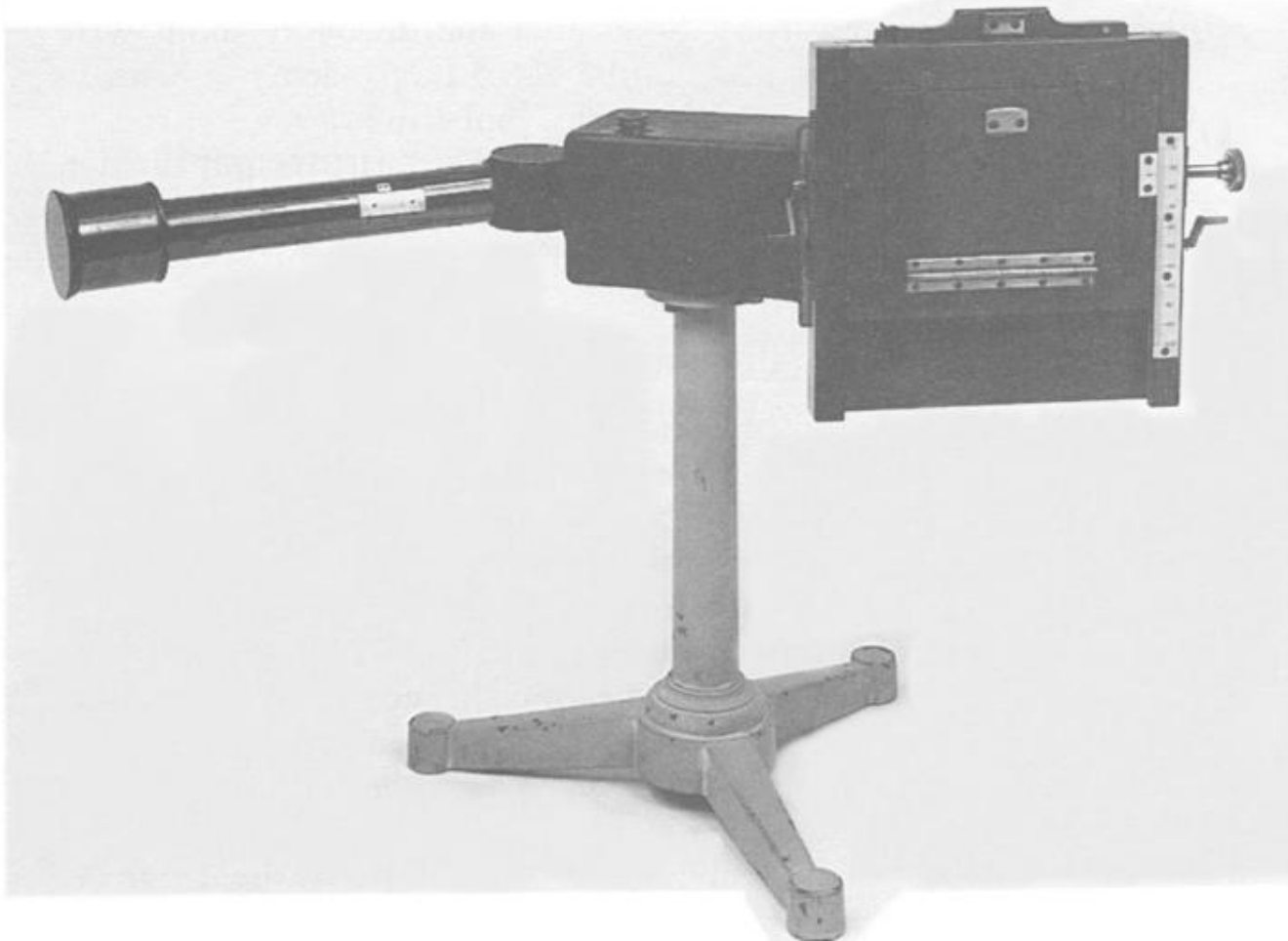
Předpověď: Adolf Smekal

A. Smekal, 'Zur Quantentheorie der Dispersion', *Naturwissenschaften* **11** (1923), 873–875.

Současný objev „kombinačního rozptylu"

G. Landsberg & L. Mandelstam, 'Eine neue Erscheinung der Lichtzerstreuing in Krystallen', *Naturwissenschaften* **16** (1928), 557–558. The full spectrum of their materials later revealed both molecular and lattice modes.

QM teorie: Georg Placzek

G. Placzek, 'Zur Theorie des Ramaneffekts', *Z. Phys.* **58** (1929), 585–594.

G. Placzek, 'Intensität und polarisation der Ramanschen Streustrahlung mehratomiger Moleküle', *Z. Phys.* **70** (1931), 84–103. Dean of Raman theorists, Placzek was a relative latecomer to the field. His 1934 review, reissued in English as *Rayleigh and Raman Scattering* (Washington D.C., U.S. Atomic Energy Commission, 1962) was the first comprehensive statement of the basic theory.

QM teorie: Georg Placzek

Intensität und Polarisation der Ramanschen Streustrahlung mehratomiger Moleküle.

Von **G. Placzek** in Utrecht.

Es wird betont, daß der Ramaneffekt an Molekülen allgemein als Folge der Wechselwirkung zwischen Kern- und Elektronenbewegung anzusehen ist. Aus dieser Auffassung ergeben sich einfache Ausdrücke für Intensität und Polarisation. Es zeigt sich, daß für die Intensität die chemische Bindung von Wichtigkeit ist: für heteropolare Moleküle ist nur ein sehr schwacher Ramaneffekt zu erwarten, der um so stärker wird, je mehr sich der Bindungstyp dem homöopolaren nähert; ferner besteht ein Zusammenhang zwischen der Intensität der einzelnen Linien und der Schwingungsform der zugehörigen Normalschwingung. Aus der Diskussion der Formeln ergeben sich ferner Bedingungen für das Auftreten von Niveaudifferenzen im Ramaneffekt, und Regeln für Intensität und Polarisation der Linien, die die Zuordnung der beobachteten Frequenzen zu bestimmten Schwingungstypen ermöglichen. — Der Vergleich mit der Erfahrung wird an den Beispielen CCl_4, CO_2, CS_2, N_2O, SO_2, C_2H_2, C_2H_4 durchgeführt, wobei sich zeigt, daß der Ramanbefund in vielen Fällen die bisherige Zuordnung bestätigt oder die Entscheidung zwischen verschiedenen strittigen Zuordnungen liefert, während er in anderen Abänderung der bisherigen Zuordnung wahrscheinlich macht.

QM teorie: Georg Placzek

$$\alpha(q_1, \ldots q) = \alpha_0 + \sum \left(\frac{\partial \alpha}{\partial q_j}\right)_0 q_j + \sum_j \left(\frac{\partial^2 \alpha}{\partial q_j^2}\right)_0 q_j^2$$

$$+ \sum_j \sum_k \left(\frac{\partial^2 \alpha}{\partial q_j \partial q_k}\right)_0 q_j q_k + \cdots, \qquad (1)$$

Zusammenfassend läßt sich somit sagen, daß auf die Intensität des Ramaneffekts im wesentlichen zwei Faktoren von Einfluß sind:

1. Die chemische Bindung in dem eben erläuterten Sinne.

2. Die Schwingungsform: in jenem Grade, in dem die zu einer Normalschwingung gehörende Kombination der Verrückungen sich dem durch (10) gegebenen Symmetrietyp nähert, wird die Intensität der entsprechenden Ramanlinie herabgesetzt, um schließlich, wenn (10) erfüllt ist, ganz zu verschwinden.

Georg Placzek

symetrie vlastních kmitů

2. *Die Gruppe AB_2*. Die Gruppe AB_2 besitzt drei Eigenschwingungen. Im Falle linearer Struktur nehmen diese die in Fig. 1 dargestellte Form an. Die Schwingung ν_2 kann im Ultraroten nicht auftreten. Die Anwendung der Auswahlregel des § 2 zeigt, daß die Schwingungen ν_1 und ν_3 die durch (10) geforderte Symmetrie besitzen; die Symmetrieoperation, die die Umkehrung sämtlicher Verrückungen bewirkt, ist eine einfache Drehung um 180^0. ν_1 und ν_3 sind daher im Ramaneffekt verboten. In der Tat fehlen diese beiden Frequenzen im Ramanspektrum aller jener Moleküle, aus deren dielektrischem Verhalten und Ultrarotspektrum auf stabförmigen Bau zu schließen ist [2] [CO_2 [3]), CS_2 [4]), N_2O [3])]; bei SO_2 hingegen, dem gewinkelte Struktur zukommt, wodurch die Auswahlverbote sowohl für Absorption als auch für Ramaneffekt wegfallen, treten alle drei Frequenzen auf [5]), in Übereinstimmung mit dem ultraroten Absorptionsspektrum [6]).
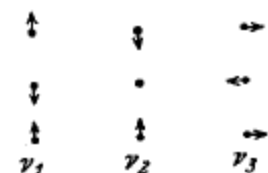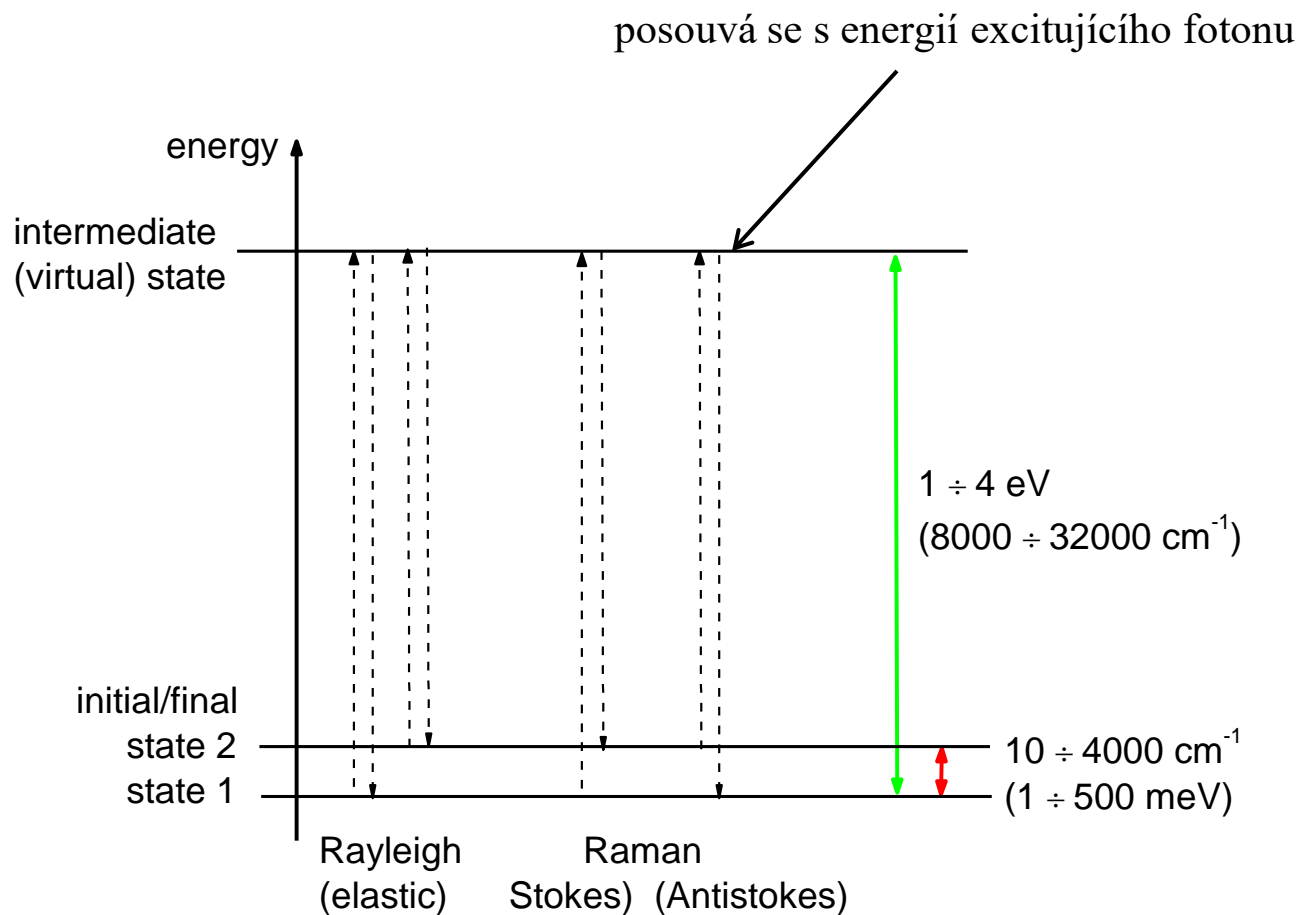

Fig. 1.
Eigenschwingungen des stabförmigen Moleküls AB_2.

Schaefer hat versucht, das Ausfallen von Ramanlinien, insbesondere der Frequenz ν_3 von CO_2, in der folgenden Weise zu begründen [7]): Der Ramaneffekt trete nur bei anharmonischer Bindung auf; bewegten sich aber nun bei einer Schwingung die Atome in symmetrischen Kraftfeldern, so müßte in der potentiellen Energie das in den Verrückungen kubische Glied verschwinden und erst das (viel schwächere) Glied mit der vierten Potenz könnte eine Anharmonizität erzeugen. Dies hätte zur Folge, daß, ebenso wie im ultraroten Absorptionsspektrum der erste Oberton, im Ramaneffekt der Grundton verschwinden müsse.

Rozptylový proces

posouvá se s energií excitujícího fotonu

energy

intermediate
(virtual) state

$1 \div 4$ eV
($8000 \div 32000$ cm^{-1})

initial/final
state 2
state 1

$10 \div 4000$ cm^{-1}
($1 \div 500$ meV)

Rayleigh
(elastic)

Raman
Stokes) (Antistokes)

Ramanův rozptyl

odlišnost od nekoherentního luminiscenčního (fluorescenčního) procesu (ten je nezávislý na excitační vlnové délce, není v antistokesově větvi)
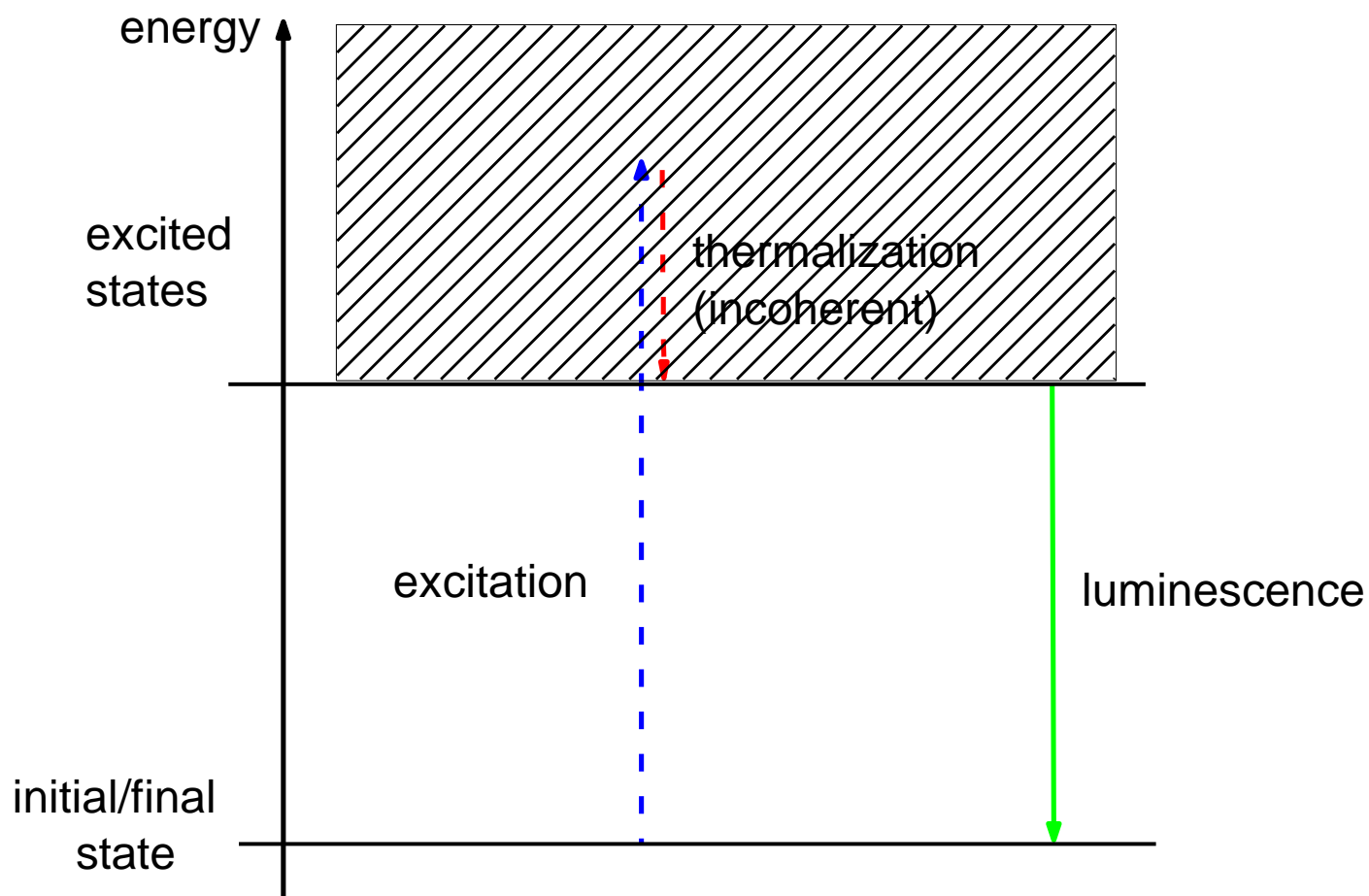
Normal vibrational modes

A molecule consisting of N atoms has $3N$ degrees of freedom;
classical equations of motion with the restoring forces proportional to the
displacements u_{kl} of the k-th atom in the l-th direction ($k=1,...,N$, $l=x,y,z$) can
be transformed into $3N$ algebraic equations with a real (dynamical) matrix, assuming
harmonic, in-phase motion of the atoms.

These equations can be solved via finding the eigenvectors $e_{kl}^{(r)}$ of the dynamical
matrix, and the corresponding eigenvalues (frequencies) $\omega^{(r)}$.
The actual displacements can be expanded in terms of the eigenvectors,

$$u_{kl} = \frac{1}{\sqrt{m_k}} \sum_r Q_r e_{kl}^{(r)},$$

where m_k is the mass of the k-th atom. The expansion coefficients are called
normal coordinates.

Normal vibrational modes – restrictions due to the symmetry

The 3*N*–dimensional vectors of the displacements form a basis for a (reducible) representation of the symmetry group, that can be decomposed in terms of the irreducible representations.

The infrared activity of a given mode requires the presence of a dipole moment, which transforms as a three-dimensional vector, forming a basis for a (reducible) representation. If an irreducible component of this representation is among the components forming the normal modes, the corresponding normal vibration is infrared active. Otherwise is the excitation of the normal mode by infrared waves forbidden by symmetry.

Listing he basis functions in the character tables is of help, because the dipole moment transforms as the vector (x,y,z).

<u>Normal vibrational modes</u> – restrictions due to the symmetry

The Raman activity of a given mode requires the presence of a nonzero derivative of the induced dipole moment with respect to the vibrational displacements; these transform as a symmetric tensor of rank 2, forming a basis for a (reducible) representation. If an irreducible component of this representation is among the components forming the normal modes, the corresponding normal vibration is Raman active. Otherwise is the Raman scattering involving the normal mode forbidden by symmetry.

Listing he basis functions in the character tables is of help, because the functions $\{x^2, y^2, z^2, xy, yz, xz\}$ form the basis for the tensorial representation.
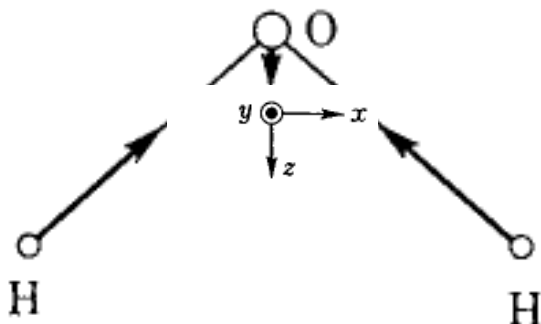
Vibrational modes of the water molecule

C_{2v} symmetry group:

E (identity), C_2 (two-fold axis z), mirror plane σ_y (xz) , mirror plane σ_x (yz)

each of the elements forms a class $\rightarrow$ 4 one-dimensional irreducible representations

Table B.10. C_{2v}

C_{2v}		Basis	E	C_2	σ_y	σ_x
A_1	Γ_1	z, x^2, y^2, z^2	1	1	1	1
A_2	Γ_2	xy	1	1	-1	-1
B_1	Γ_3	x, xz	1	-1	1	-1
B_2	Γ_4	y, yz	1	-1	-1	1

9 degrees of freedom, 9-6=3 vibrational ones

Let us first count the number of atoms N_R which are not moved by the symmetry operation R (only these atoms are relevant for the characters of representations, since they contribute non-vanishing diagonal elements):

C_{2v}	E	C_2	σ_y	σ_x
N_R	3	1	3	1

Vibrational modes of the water molecule

Next, a (proper) rotation about the z axis through an angle α transforms the displacements from equilibrium positions (actually, any vector) according to

$$\begin{bmatrix} u'_x \\ u'_y \\ u'_z \end{bmatrix} = \begin{bmatrix} \cos\alpha & -\sin\alpha & 0 \\ \sin\alpha & \cos\alpha & 0 \\ 0 & 0 & 1 \end{bmatrix} \begin{bmatrix} u_x \\ u_y \\ u_z \end{bmatrix}.$$

Its contribution to the character, independent of the orientation of the axis, is

$$\chi_{vect}(R_\alpha) = 1 + 2\cos\alpha.$$

Improper rotations iR_α, consisting of proper rotations and inversion i, contribute

$$\chi_{vect}(iR_\alpha) = -1 - 2\cos\alpha.$$

Using the allowed angle for the crystallographic point groups, we obtain the contributions (for the water molecule, we need the colored entries only):

E	C_6	C_4	C_3	C_2	i	S_6	S_4	S_3	$S_2=\sigma$
3	2	1	0	-1	-3	-2	-1	0	1

<u>Vibrational modes of the water molecule</u>

All the atoms left unmoved by the symmetry operation R contribute the same value, $\chi_{vect}(R)$, to the character of the $3N$-dimensional representation based on the $3N$-dimensional vector of displacements:

$$\chi(R) = N_R \chi_{vect}(R).$$

We arrive at the sought (the last row) character table:

C_{2v}	E	C_2	σ_y	σ_x
N_R	3	1	3	1
$\chi_{vect}(R)$	3	-1	1	1
$\chi(R)$	9	-1	3	1

Not to forget: the corresponding representation contains three translation and rotation modes of the molecule as a whole.

Vibrational modes of the water molecule

The coordinates of the translation form a basis of the 3-dimensional representation with the character $\chi_{trans}(R)=\chi_{vect}(R)$. The rotation is described by an axial vector (no change of sign on inversion); consequently, the character is $1+2\cos(\alpha)$ for both proper and improper rotations by the angle α. We can subtract the two irrelevant motions from the character χ to obtain the wanted description of vibrations:

C_{2v}	E	C_2	σ_y	σ_x
$\chi(R)$	9	-1	3	1
$\chi_{trans}(R)$	3	-1	1	1
$\chi_{rot}(R)$	3	-1	-1	-1
$\chi_{vibr}(R)$	3	1	3	1

The 3-dimensional representation χ_{vibr} is reducible.

<u>Vibrational modes of the water molecule</u>

The irreducible components are easily found.

1. One of them must be A_1, we subtract it:

C_{2v}	E	C_2	σ_y	σ_x
$\chi_{vibr}(R)$	3	1	3	1
A_1	1	1	1	1
$\chi_{vibr}(R)$-A_1	2	0	2	0

2. The projection of the rest on A_1 is nonzero; the latter is contained once more, we subtract it:

C_{2v}	E	C_2	σ_y	σ_x
$\chi_{vibr}(R)$-A_1	2	0	2	0
A_1	1	1	1	1
$\chi_{vibr}(R)$-$2A_1$	1	-1	1	-1

The rest is B_1 and we arrive at the decomposition of $2A_1 + B_1$.

Vibrational modes of the water molecule
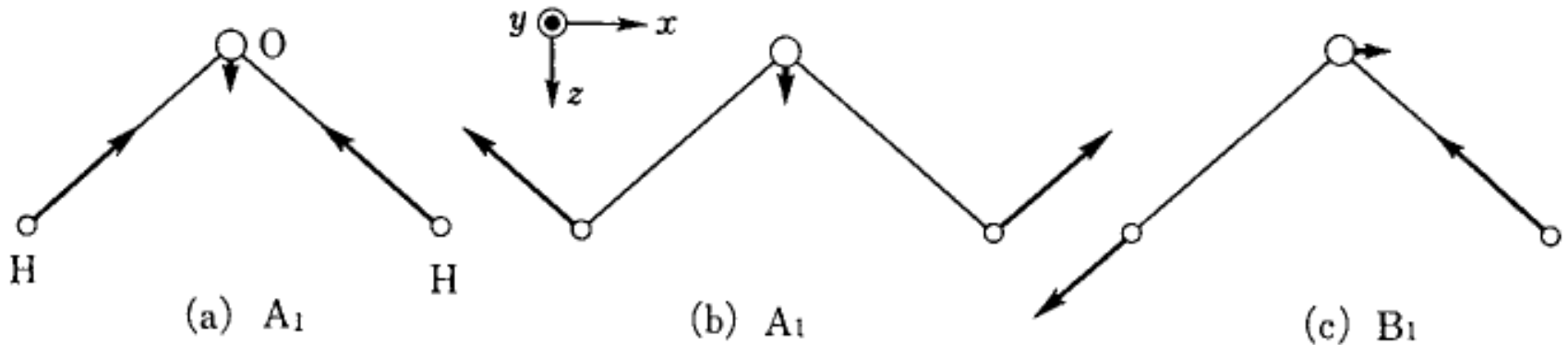
The symmetry analysis classifies the three normal modes:

Fig. 10.3. Normal modes of the H₂O molecule. The arrows indicate the displacements

(a) 3651.7 cm⁻¹, symmetric stretching, monotonic dependence of the polarizability on the normal coordinate → nonzero slope at equilibrium (Raman active), dipole moment along z (IR active);

(b) 1595 cm⁻¹, bending, low frequency due to small restoring forces, monotonic dependence of the polarizability on the normal coordinate → nonzero slope at equilibrium (Raman active), dipole moment along z (IR active);

(a) 3755.8 cm⁻¹, asymmetric stretching, monotonic dependence of the polarizability on the normal coordinate → nonzero slope at equilibrium (Raman active), dipole moment along z (IR active).

Vibrational modes of the H_2O molecule - overview Herzberg

TABLE 60. INFRARED AND RAMAN BANDS OF H_2O VAPOR.

ν_{vacuum},[35] observed (cm^{-1})	Band type[36]	Upper state[37] $v_1\ v_2\ v_3$	Species	ν, calculated (cm^{-1})	References
1595.0	I. $\parallel$[38] v.s.	0 1 0	A_1	1595.0*	(704) (665)
3151.4	I. $\parallel$ m.	0 2 0	A_1	3151.0*	(704) (665)
3651.7[39]	I. $\parallel$ s., R. s.	1 0 0	A_1	3650.0*	(667) (475) (716) (135)
3755.8	I. $\perp$[40] v.s.	0 0 1	B_1	3755.41*	(704) (612) (667)
5332.0	I. $\perp$ m.	0 1 1	B_1	5330.6	(704) (702) (612) (667)
6874	I. $\perp$ w.	0 2 1	B_1	6866.8	(234a)
7251.6	I. $\perp$ m.	1 0 1	B_1	7250.4	(702) (612) (667)
8807.05	P.I. $\perp$ s.	1 1 1	B_1	8805.5	(612) (591)
10613.12	P.I. $\perp$ s.	2 0 1	B_1	10613.12*	(612) (130)
11032.36	P.I. $\perp$ m.	0 0 3	B_1	11032.36*	(612) (130)
12151.22	P.I. $\perp$ m.	2 1 1	B_1	12148.5 $\}$*	(612) (130)
12565.01	P.I. $\perp$ v.w.	0 1 3	B_1	12567.7	(612) (130)
13830.92	P.I. $\perp$ w.	3 0 1	B_1	13830.92*	(612) (130)
14318.77	P.I. $\perp$ w.	1 0 3	B_1	14318.77*	(612) (333)
15347.91	P.I. $\perp$ v.w.	3 1 1	B_1	15346.3 $\}$*	(612) (333)
15832.47	P.I. $\perp$ v.w.	1 1 3	B_1	15834.1	(612) (333)
16821.61	P.I. $\perp$ v.w.	3 2 1	B_1	16822.7	(612) (333)
16899.01	P.I. $\perp$ v.w.	4 0 1	B_1	16894.3	(612) (333)
17495.48	P.I. $\perp$ v.w.	2 0 3	B_1	17482.6	(612) (333)

[35] The frequencies below 8000 cm^{-1}, with the exception of the band 6874 cm^{-1}, are those of Nielsen (665) (667) reduced to vacuum (assuming that he has not reduced them); the other frequencies are those of Mecke and his co-workers (612) (130) (333) which are stated to be ν_{vacuum}.

[36] $\parallel$ and $\perp$ refer here to the direction of the variable part of the dipole moment with respect to the symmetry axis. Nielsen (665) (667) uses the opposite nomenclature, taking $\parallel$ and $\perp$ to mean parallel and perpendicular to the axis of least moment of inertia.

[37] The lower state for all observed bands is 0, 0, 0 A_1.

[38] A Raman band has been observed by Johnston and Walker (475) in H_2O vapor at 1648 cm^{-1} but has not been confirmed by Rank, Larsen, and Bordner (716). However, such a Raman line has definitely been established in liquid H_2O [see Rao and Koteswaran (722)].

[39] This is the wave number of the zero line of the infrared band. The center of the Raman band of H_2O vapor has been observed at 3654.5 cm^{-1} by Bender (135). Rank, Larsen, and Bordner (716) give a doublet with frequency shifts 3646.1 and 3653.9 cm^{-1}.

Examples of Raman spectra - (liquid) water

(Ph. Valee et al., Journal of Molecular Structure, 2003, 651-653: 371-379)
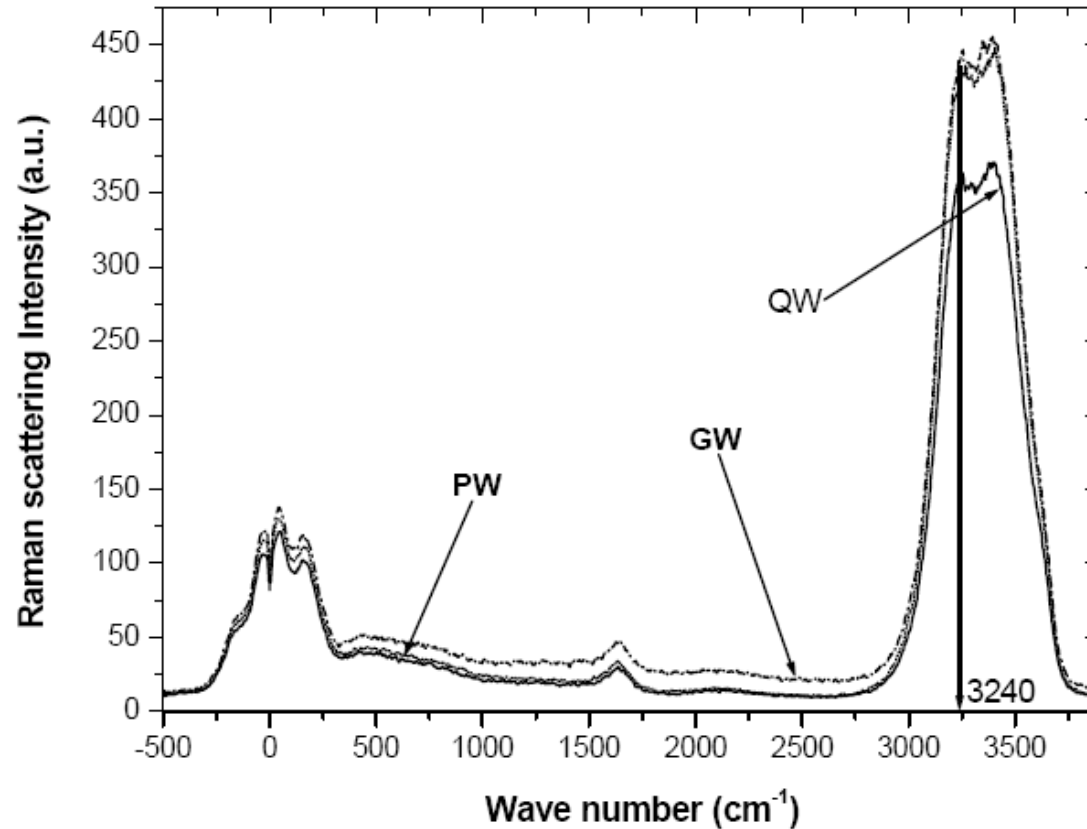

Figure 1 : Full Raman (excitation 514.5 nm) scattering spectra of SEROMED water samples in quartz glass (QW), polypropylene (PW) and soda-lime glass type III (GW) tubes.

Examples of Raman spectra - water

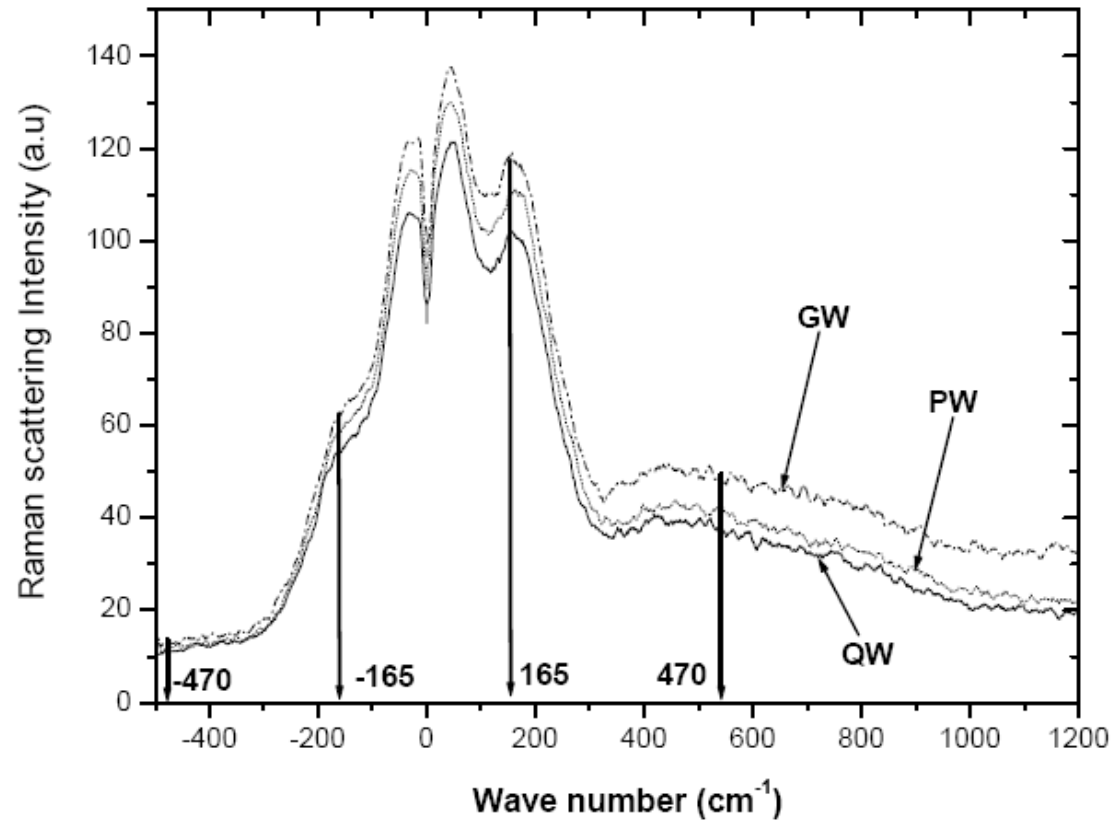(Ph. Valee et al., Journal of Molecular Structure, 2003, 651-653: 371-379)

Figure 3: Expansion of Raman spectra of Figure 1 in the low frequency domain (-500 to 1200 cm^{-1}).

Examples of Raman spectra -

Calcite

(Porto et al., Phys. Rev. 147, 608 (1966))

The experimental apparatus has been described elsewhere[18]; it consists of a 50-mW He-Ne laser ($\lambda = 6328$ Å) chopped at 400 cps, the light of which passes through a focusing lens or directly through apertures into the crystal. Scattered light is collected at 90° from the incident beam, focused into an $f/6.8$ grating spectrometer and detected by an $S20$ photomultiplier. The photomultiplier signal is amplified in a lock-in amplifier and recorded. A polarizer in front of the entrance slit is used to observe the polarization of the scattered radiation. The slit widths used in our measurements correspond to about 7 cm^{-1} and the integration time of the recordings was 3 sec.
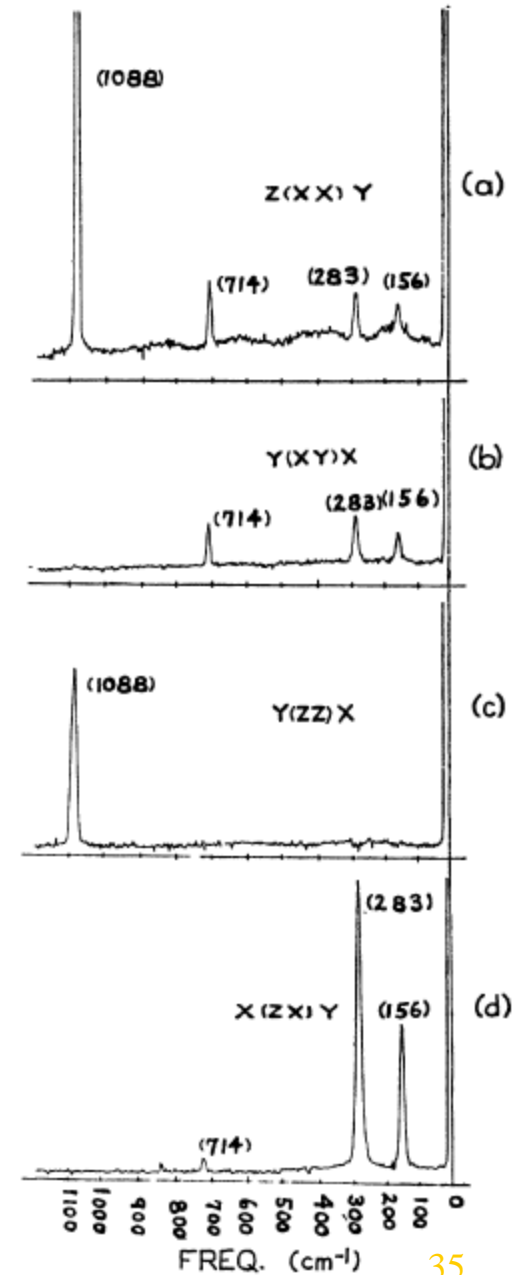
FIG. 1. Raman spectrum of calcite. The notation $x(zx)y$ indicates the spectrum with incident light directed along the *crystal* x axis and polarized along the z axis; the direction of observation of the x-polarized scattered light is the y axis.

Note:

the 1088 cm^{-1} A_{1g} mode corresponds probably to the "$\lambda_1 = 9.1$ μ Trabant" observed by Landsberg&Mandelstam
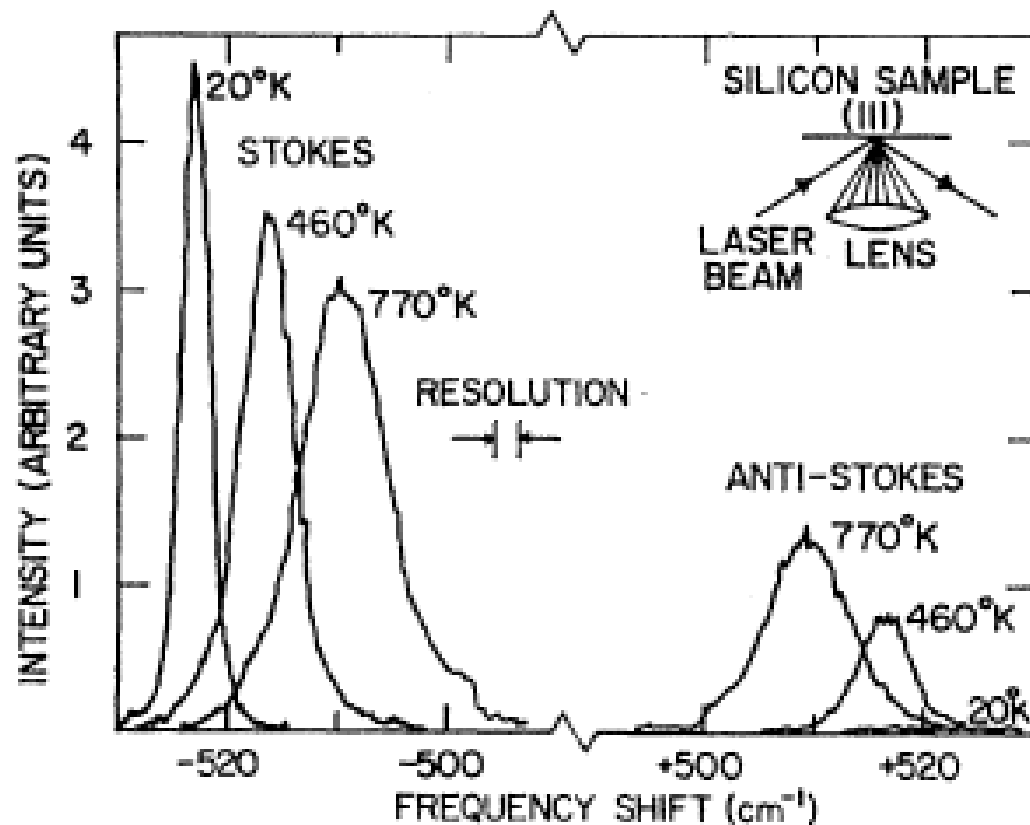
Examples of Raman spectra - intrinsic silicon

FIG. 1. First-order Raman spectra of silicon observed at 20, 460, and 770°K with an instrumental resolution of ~2 cm⁻¹. Insert shows the scattering geometry used.

Examples of Raman spectra - heavily doped p-type silicon
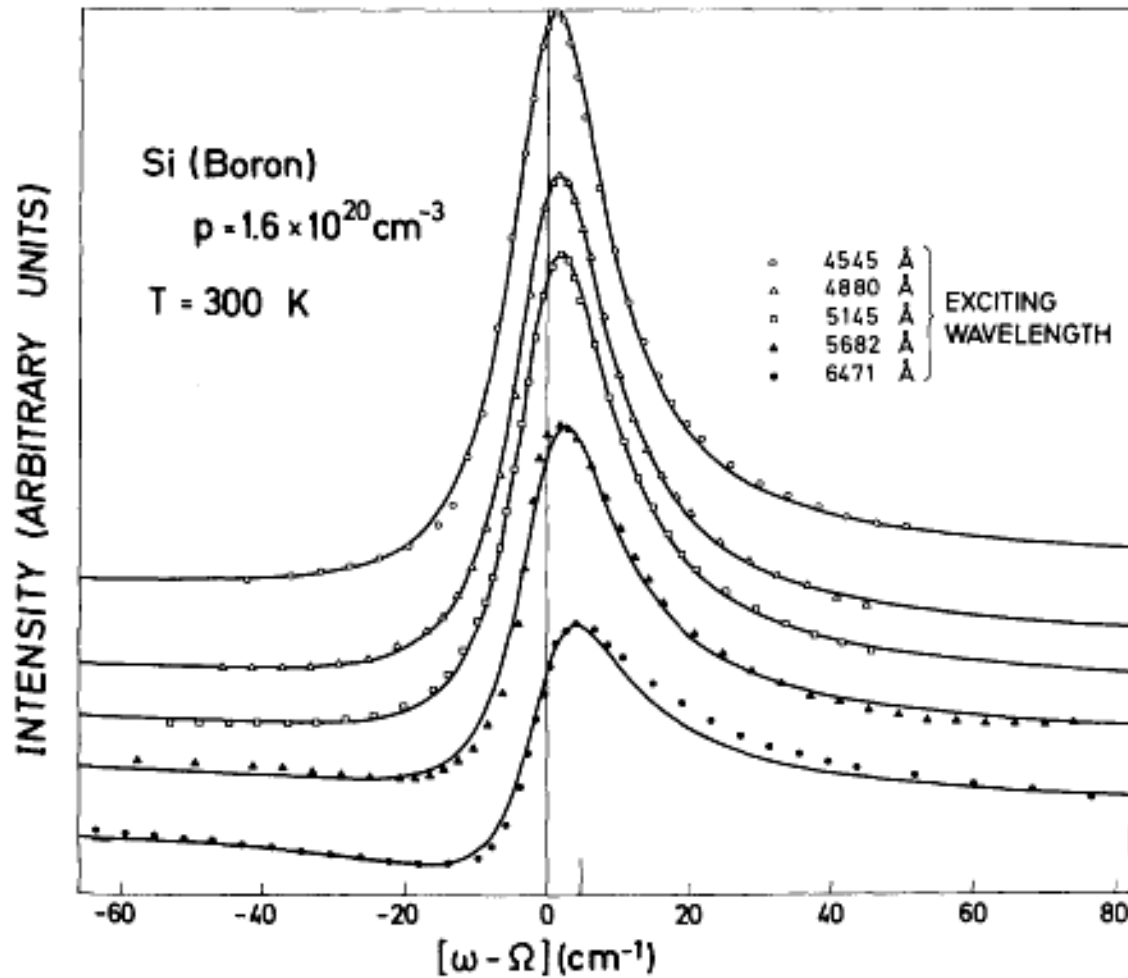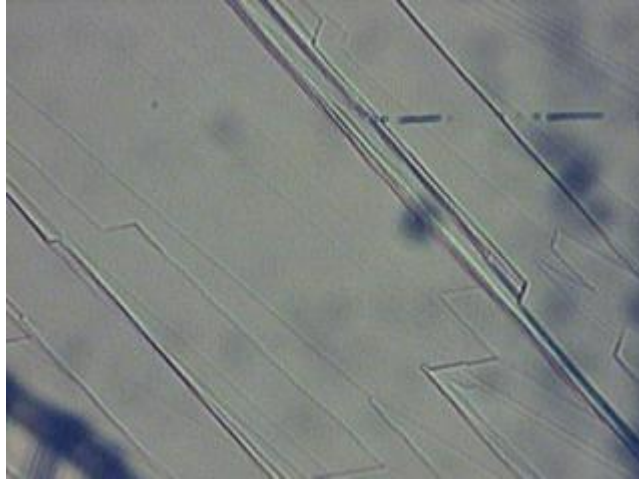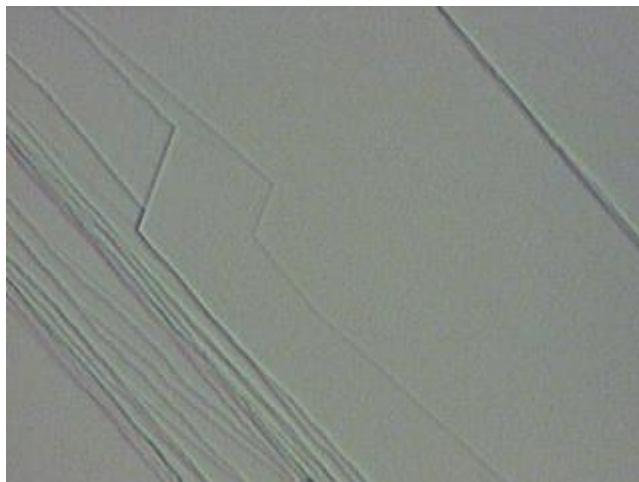
(M.V. Klein, Light Scatt. Sol. I, p. 173)

Fig. 4.9. Room temperature Raman spectra for p-type Si [4.56, 58]. For easier viewing the curves have been shifted vertically with respect to one another. The points are experimental data; the lines are calculated curves using (4.49a) with constant ϱ, R

Raman spectra of "topological insulators" Bi2Te3, Bi2Se3
ÚFKL 2012-13, epilayers on BaF2 (JKU Linz)
defects, steps on the substrates

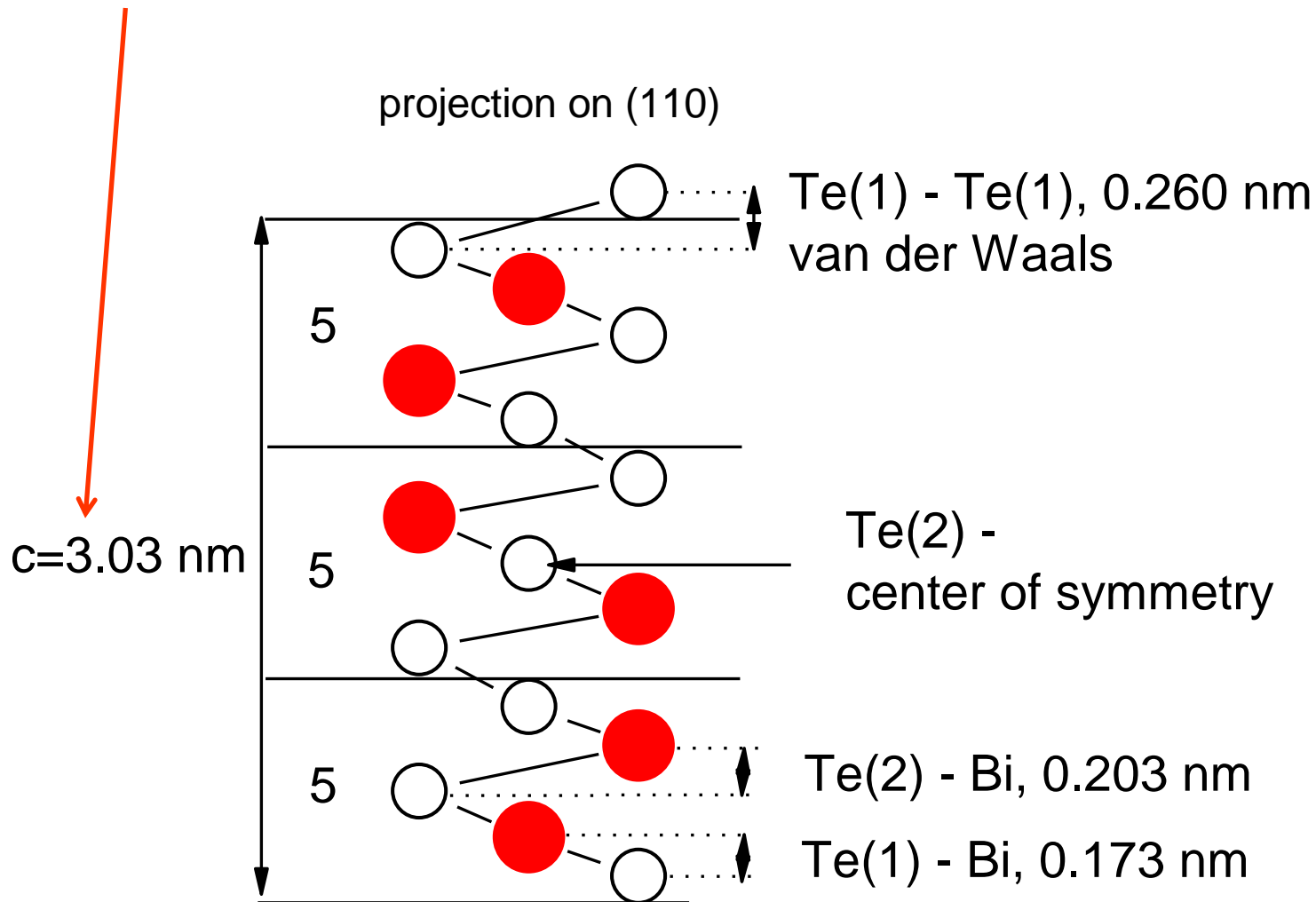MBE2805 backside 5x


MBE2805 backside 20x

Crystalline Bi2Te3, 3 quintuples

projection on (110)

Te(1) - Te(1), 0.260 nm
van der Waals

c=3.03 nm

5

5

5

Te(2) -
center of symmetry

Te(2) - Bi, 0.203 nm

Te(1) - Bi, 0.173 nm

Bi_2Te_3 stacking sequence: 3x[Te(1)-Bi-Te(2)-Bi-Te(1)]

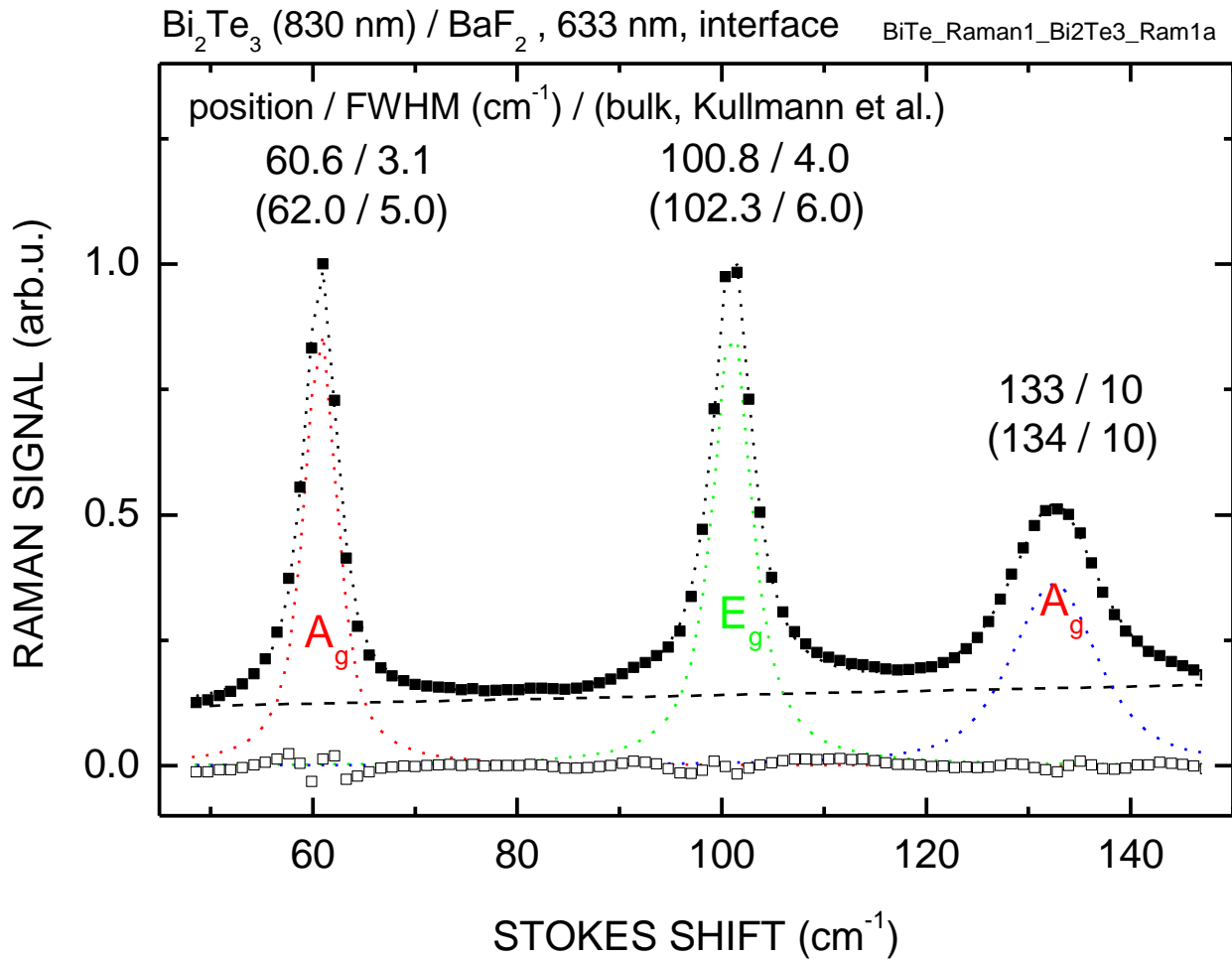# Raman spectra, backscattering geometry, unpolarized

<u>633</u> and 514 nm excitation, two possibilities

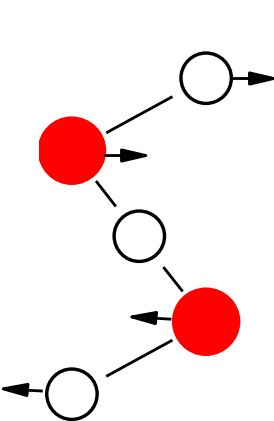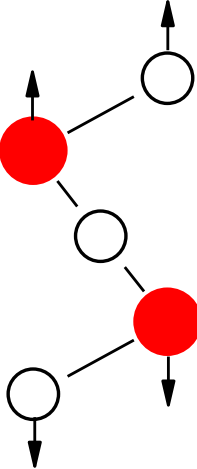**BaF$_2$ substrate (~1 mm thick) <u>transparent</u> for exciting and scattered light**
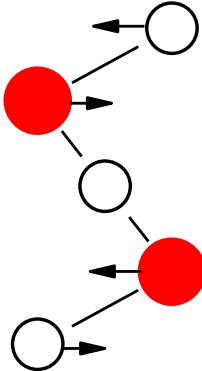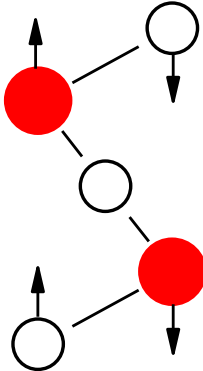
negligible overlap of the spectra of film and substrate

Renishaw In-Via

"front side"

"back side"

lens

film

BaF$_2$

BaF$_2$
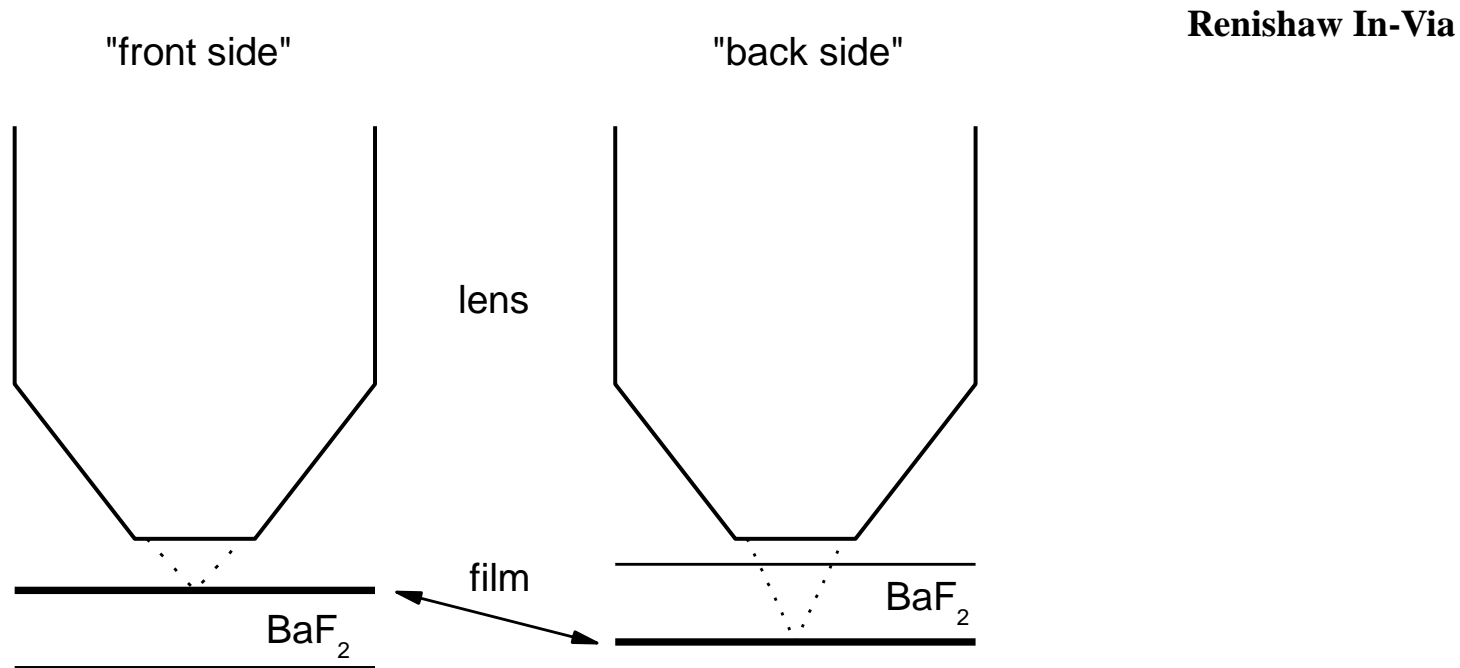
Raman spectra, 3 narrow Gaussian profiles on a flat background (when measured at the interface), very slight asymmetry

Bi_2Te_3 (830 nm) / BaF_2 , 633 nm, interface   BiTe_Raman1_Bi2Te3_Ram1a

position / FWHM (cm^{-1}) / (bulk, Kullmann et al.)

60.6 / 3.1
(62.0 / 5.0)

100.8 / 4.0
(102.3 / 6.0)

133 / 10
(134 / 10)

RAMAN SIGNAL (arb.u.)

A_g

E_g

A_g

STOKES SHIFT (cm^{-1})

Identification of normal modes (gerade)

	very weak		61	101	133	cm^{-1}
Chis et al. (2012)		42.1	64.2	112.3	139.2	

first-principles

DFT & DFPT

(perturbation th.)

$E_g(1)$	$A_{1g}(1)$	$E_g(2)$	$A_{1g}(2)$
50.6	71.1	118.5	128.3 cm^{-1}

Jenkins et al., 1972, 9 adjustable parameters, fitting measured elastic moduli

Bi_2Te_3 Raman modes

BiTe - three doublets:

633 nm

BiTe23-11_Comp23-11d

Figure shows Raman spectrum of Bi_1Te_1 MBE2882 measured at 633 nm, with peaks labeled 58.5, 60.4, 92.7, 101.7, 123.7, 131. Curves labeled "subs" and "film". X-axis: STOKES SHIFT (cm^{-1}), Y-axis: RAMAN SIGNAL (arb.u.).
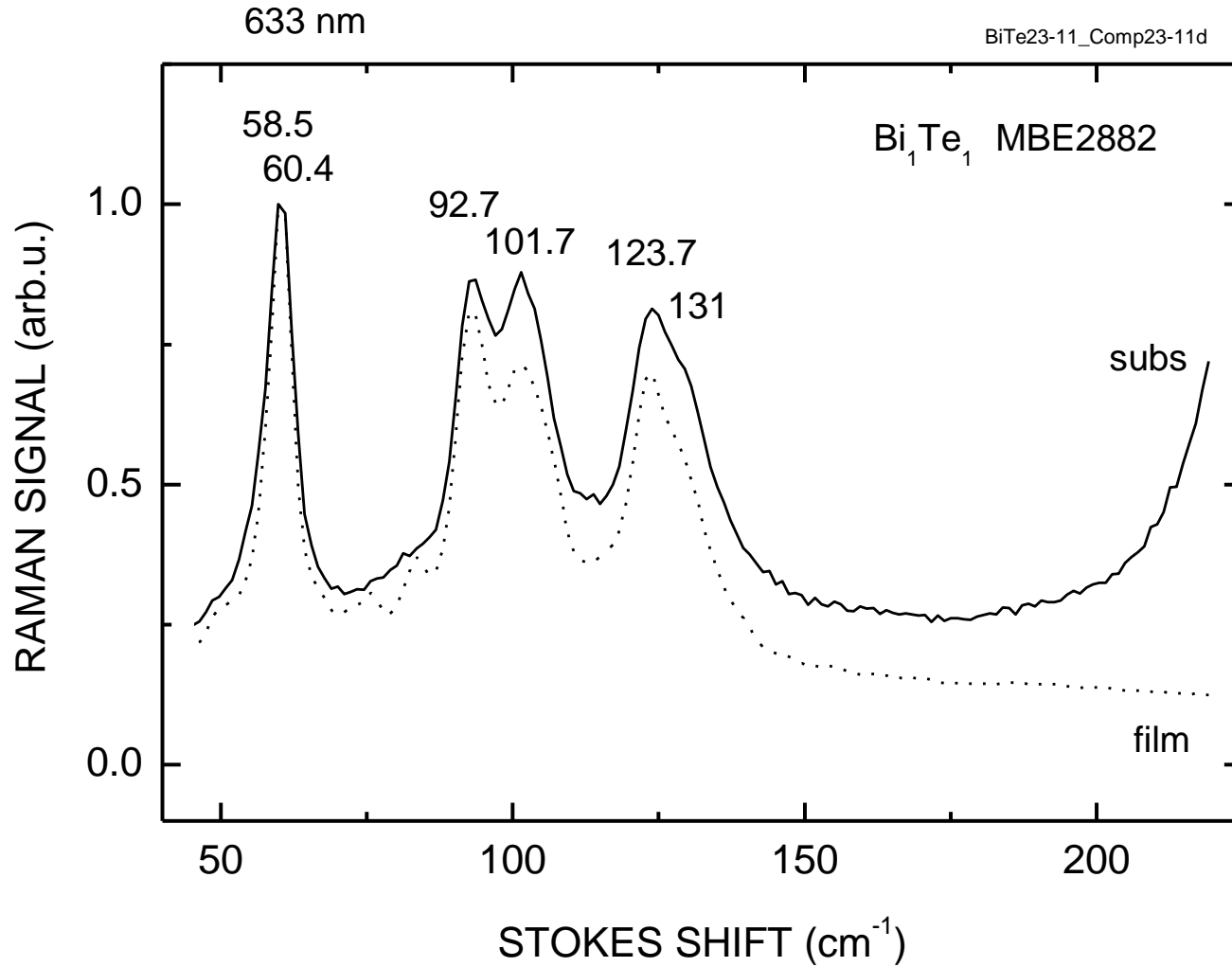
The lower symmetry of BiTe quintuplets

(the interlayer spacings in Angstroems):

Te1

Te1
Bi1
Te2
Bi2
Te3

Bi3
Bi3   2.040
                   1.131
Te3
                          1.870
Bi2
                   1.822
Te2
                   2.177
Bi1
Te1   1.656
                   2.650

7   **3**
                            different spacings

                          1.729 Bi Te1
                   2.032
                   2.032   Te2
                          1.729 Bi
                                      Te1
                   2.598

BiTe | **Bi$_2$Te$_3$**
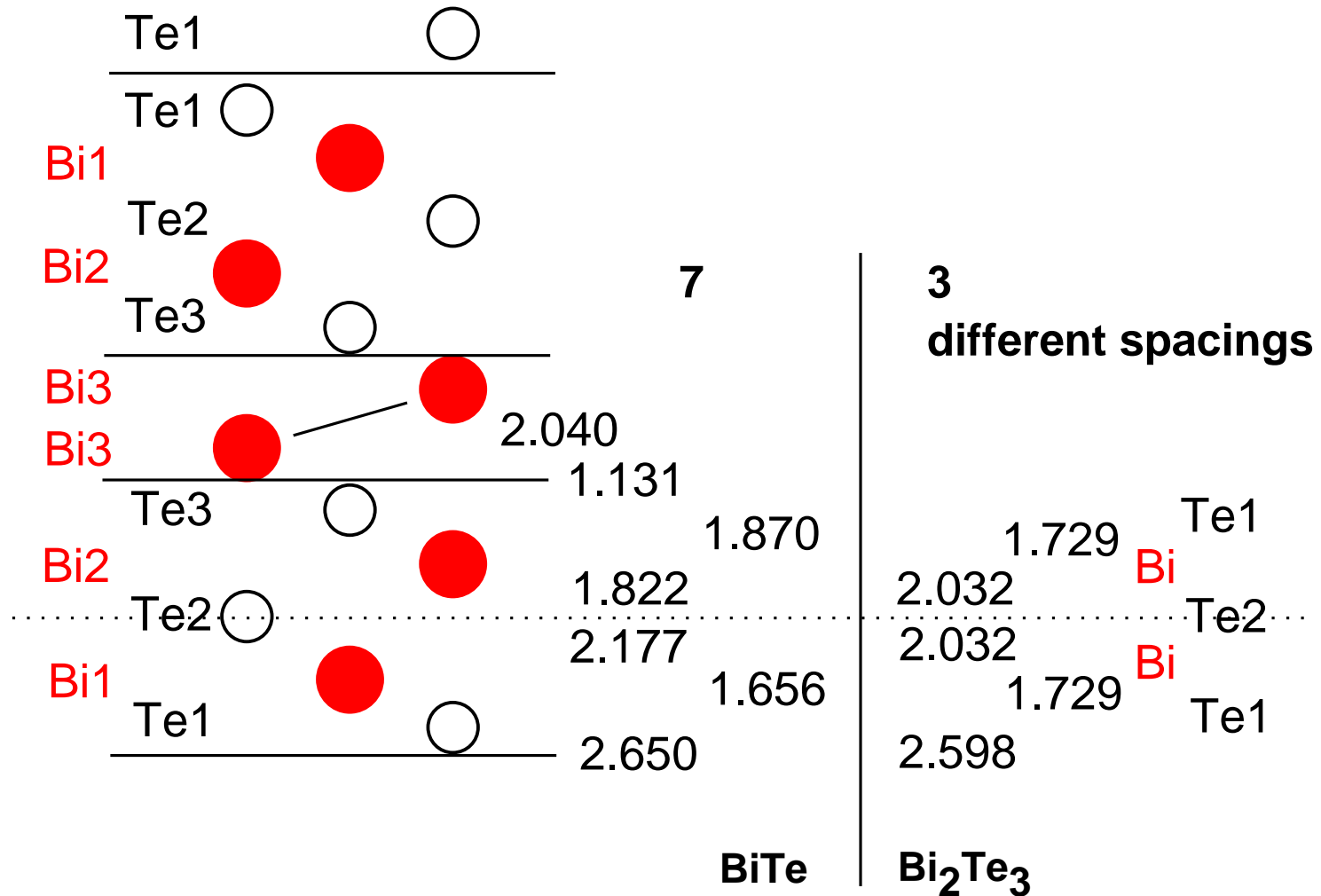
Several weaker bands seen in the detailed comparison, found also in the spectra of thick films taken from the surface;

deviations from perfect crystal stronger <u>at the surface</u>;

the growth need not end with a complete cell of Bi_2Te_3 (3.03 nm)

633 nm, surface
BiTe_RamanThin_B830-22sdd

Bi_2Te_3 MBE2780 830 nm
Bi_2Te_3 MBE2918   22 nm
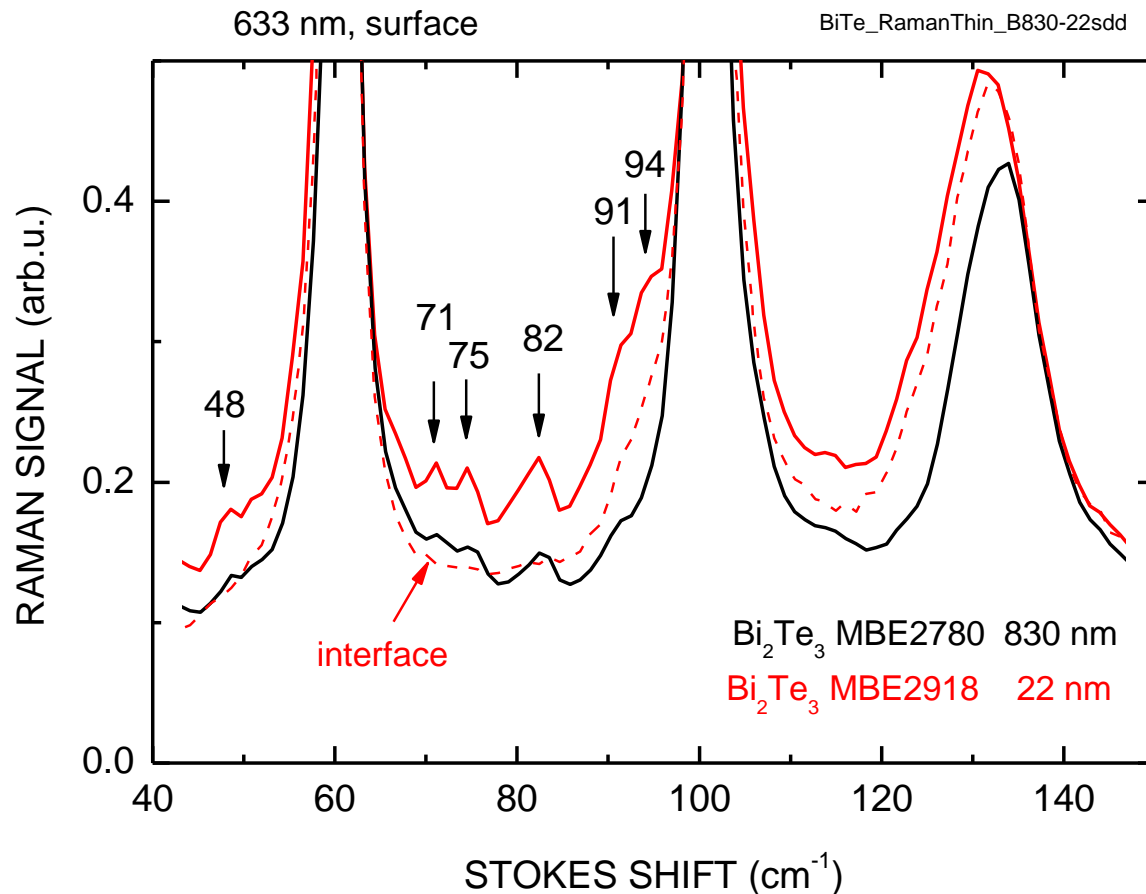
three Bi2Se3 bands

about sqrt(127.6/79)=1.27 times higher in frequencies than Bi_2Te_3

BiSe_2013_04_30_TeSe